Brute-force solvent suppression for DNP studies of powders at natural isotopic abundance

Pierre Thureau, Marie Juramy, Fabio Ziarelli, Stéphane Viel, Giulia Mollica

Brute-force solvent suppression for DNP studies of powders at natural isotopic abundance

Pierre Thureau,[†] Marie Juramy,[†] Fabio Ziarelli,[‡] Stephane Viel.[†,¶] and Giulia Mollica[,†]*

[†]Aix Marseille Univ, CNRS, ICR, Marseille, France

[¶]Institut Universitaire de France, Paris, France

[‡]Aix Marseille Univ, CNRS, Centrale Marseille, FSCM, Marseille, France

Corresponding Author

giulia.mollica@univ-amu.fr

Abstract

A method based on highly concentrated radical solutions is investigated for the suppression of the NMR signals arising from solvents that are usually used for dynamic nuclear polarization experiments. The presented method is suitable in the case of powders, which are impregnated with a radical-containing solution. It is also demonstrated that the intensity and the resolution of the signals due to the sample of interest is not affected by the high concentration of radicals. The method proposed here is therefore valuable when sensitivity is of the utmost importance, namely samples at natural isotopic abundance.

Keywords

Dynamic nuclear polarization; Natural isotopic abundance; Sample preparation; Powder; Solvent suppression

Highlights

- Highly concentrated radical solutions can be used to suppress the signal of the solvent
- No impact on signal-to-noise ratio and resolution
- The procedure is efficient for both aqueous and organic solvents

1. Introduction

The recent development of high-field dynamic nuclear polarization (DNP) has enabled a wide range of molecular systems to be thoroughly investigated.[1-16] These results have been obtained thanks to the development of hardware,[17-25] polarizing agents,[26-33] and theory.[34-41] Among these developments, the study of samples at natural isotopic abundance thrived,[42-46] especially as a result of efficient methodologies for sample preparation. Indeed, Rossini *et al.* have demonstrated that powders can be impregnated with a radical-containing solution,[47] where the polarizing agent (PA) remains at the surface of the powder particles and the DNP-enhanced ^{1}H polarization is transferred to the core of the particle through ^{1}H-^{1}H spin-diffusion.[48] This approach yielded large DNP sensitivity enhancements, which allowed samples at natural isotopic abundance to be fully characterized. Morevover, this methodology preserves the resolution of the NMR spectra because the PA remains distant from the nuclear spins that eventually contribute to the detected NMR signal.

A drawback of this method is that the solvent used to dissolve the PA is strongly enhanced by DNP, which usually results in a large solvent signal observed in the DNP-enhanced ^{1}H-^{13}C CP NMR spectra of impregnated samples. Several methods have been proposed to suppress this signal, such as solvent-free preparation methods,[49-51] relaxation filters[52] or dipolar dephasing.[53] The main advantage of these solvent-suppression methods is their versatility (although the method based on dipolar dephasing requires a triple-channel probe). In fact, these methods can be applied to different kinds of samples, such as frozen solutions,[54] porous materials[55] or impregnated powders. Unfortunately, methods based on relaxation filters or dipolar diphasing not only affect the intensity of the solvent signal but also the intensity of the signals belonging to the sample under study. The resulting loss in signal intensity may be significant and could prove detrimental to the overall signal-to-noise ratio of the DNP-enhanced NMR spectra, especially for samples at natural isotopic abundance. In addition, this intensity reduction may not be uniform for the different resonances of the sample under study.

In this contribution, we investigate the influence of using highly concentrated radical solutions when recording DNP-enhanced spectra on impregnated powders. More specifically, we demonstrate that increasing the concentration of radicals allows the signal of the solvent to be

effectively suppressed, without affecting the intensity or the resolution of the signals due to the sample of interest. The methodology proposed here is illustrated on samples that were impregnated either with an organic or an aqueaous radical-containing solution.

2. Results and Discussion

Figure 1 shows the ^{1}H-^{13}C CP MAS spectra of 3-aminobenzoic acid, which has been impregnated with two distinct solutions of TEKPol in 1,1,2,2-tetrachlroethane (TCE), namely 17 mM and 80 mM. Typically, the usual concentration of a radical solution used for incipient wetness impregnation is ~16 mM,[47, 56] which is significantly less than the concentration of 80 mM used in this study.

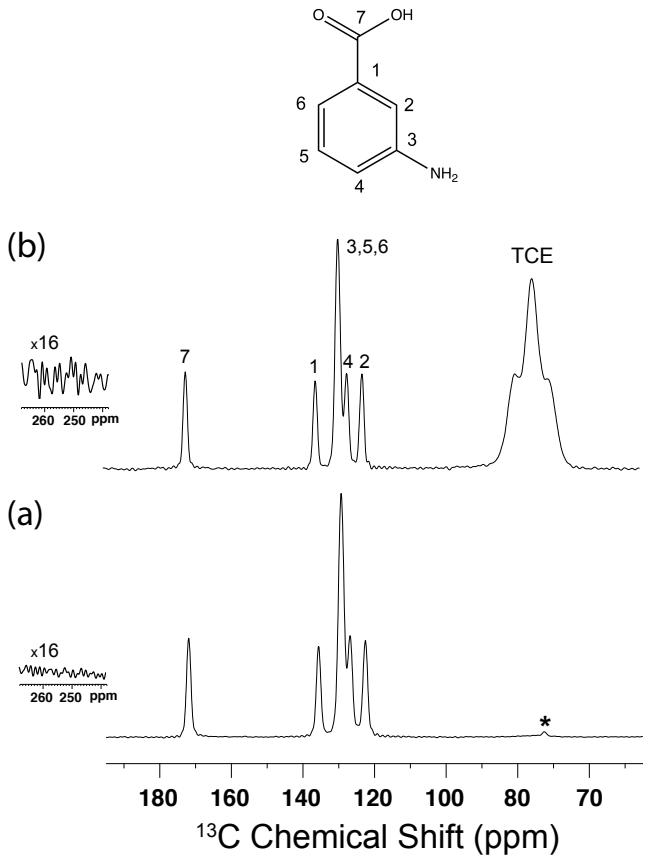

Figure 1: DNP-enhanced NMR ^{1}H-^{13}C CP MAS spectra of 3-aminobenzoic acid as a powder and impregnated with a TCE solution of TEKPol at (a) 80 mM, and (b) 17 mM. Both spectra were recorded using a relaxation delay of 10 s, at a temperature of 108 K and with a MAS frequency of 10 kHz. The

experimental time to record each spectram was 60 s. The noise for each spectrum is shown in the inset. (The symbol * indicates a spinning side band).

Interestingly, both spectra shown in Figure 1 have comparable resolution but the signal arising from TCE is not observable in the spectrum recorded for the sample impregnated with the TCE solution of TEKPol at 80 mM (Figure 1a). In fact, the high concentration of the PA leads to strong paramagnetic relaxation that shortens the apparent relaxation times of the nuclear spins close to the PA. In the case of incipient wetness impregnation of powders, the relaxation of the nuclei belonging to the solvent is thus considerably affected by this paramagnetic relaxation, while the relaxation of the remote nuclei belonging to the core of the powder particle is much less altered.

The ^{1}H-^{13}C CP MAS spectra of 3-aminobenzoic acid recorded at a temperature of ~108 K and shown in Figure 2 underline the impact of the solvent and PA on the spectral linewidths of the NMR signal after incipient wetness impregnation. Interestingly, Figure 2 shows that the broadening of the NMR signal arises mainly from the presence of the solvent rather than from the presence of the PA. In fact, the ^{1}H-^{13}C CP MAS spectra shown in Figure 2a and 2b, which were both recorded after impregnation with TCE, have nearly identical spectral linewidths, despite the fact that the spectrum shown in Figure 2b has been recorded in the absence of PA. It should also be noted that the ^{1}H-^{13}C CP MAS spectrum shown in Figure 2c and recorded for the pure powder displays slightly narrower linewidths. This results confirms the minor impact of the PA on the ^{13}C coherence lifetimes (T_2'), and hence on the resolution of NMR spectra of samples that have been impregnated with a high concentration of PA.

Table 1: Relaxation properties, DNP signal enhancements and sensitivity (expressed as the S/N of the ^{13}C CPMAS spectrum normalized to the square root of the experimental time) measured for 3-aminobenzoic acid impregnated with a TCE solution of TEKPol.

Concentration of TEKPol in TCE (mM)	T_1^a(^{1}H) and T_1^b(^{1}H) [a] (s)	A	B	T_2'(^{13}C) [b] (ms)	ε_{CP}	S/N x $t^{1/2}$
17	2.4±0.1 and 105±7	0.40	0.60	38±3	26	12
80	0.60±0.1 and 45±5	0.35	0.65	37±3	76	53

[a]Data obtained with a biexponential fitting of the form $S(\tau)= A \exp[-\tau/T_1^a]+ B \exp[-\tau/T_1^b]$

[b]Measured for the fastest decaying signal, *i.e.* the C2 resonance.

Furthermore, a higher sensitivity (expressed as the S/N of the ^{13}C CPMAS spectrum normalized to the square root of the experimental time) is obtained for the sample impregnated with the 80 mM TEKPol/TCE solution with respect to the sample impregnated with the 17 mM TEKPol/TCE solution. In fact, as shown in Table 1, both samples have comparable ^{13}C coherence lifetimes (T_2') but the ^{1}H longitudinal relaxation time (T_1) and the DNP signal enhancement ($\varepsilon_{C,CP}$) are more favorable for the sample impregnated with the 80 mM TEKPol/TCE solution. As a result, the overall sensitivity enhancement is ~4 times higher for the sample impregnated with the 80 mM TEKPol/TCE solution. This result is in full agreement with the previous results reported by Mollica *et al.* for theophylline, where the maximal overall sensitivity was obtained for the powder impregnated with a 66 mM solution of TEKPol in EtBr4.[44]

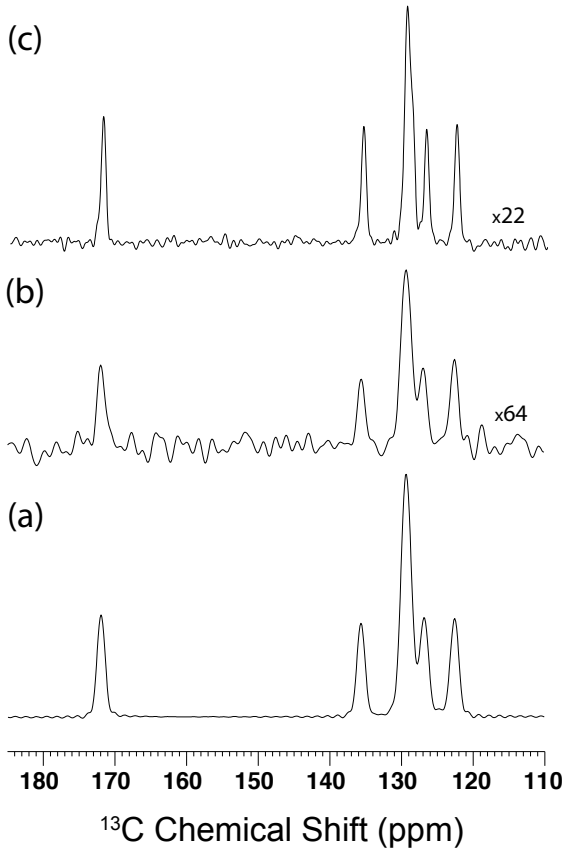

Figure 2: ^{1}H-^{13}C CP MAS spectra of 3-aminobenzoic acid recorded with microwaves irradiation on (a) the powder impregnated with a TCE solution of TEKPol at 80 mM, (b) the powder impregnated with TCE, and (c) the pure powder. All spectra were recorded at a temperature of 108 K and a MAS frequency of 10 kHz. The experimental time to record each spectrum was 80 s.

It should also be noted that identical measurements have been performed for two additional radical concentrations, namely 30 mM and 55 mM. Interestingly, the signal of TCE was quenched for the sample impregnated with the 55 mM radical solution while the signal of TCE was still observed in the spectrum recorded for the sample impregnated with the 30 mM solution. Furthermore, we observed that the highest sensitivity per unit time was obtained for the sample impregnated with the 80 mM radical solution. The evolution of the DNP enhancement ε_{CP} and the S/N per experimental time are given in the Supporting Information.

These favorable experimental conditions allowed two-dimensional NMR experiments to be carried out for the sample of 3-aminobenzoic acid at natural isotopic abundance. For example, Figure 3 shows the double quanta (DQ)-single quantum (SQ) ^{13}C-^{13}C correlation 2D spectrum obtained for the sample impregnated with the 80 mM TEKPol in TCE. In this experiment, the method of Dekhil *et al.* has been used to reintroduce the ^{13}C-^{13}C dipolar coupling during a short dipolar recoupling time (0.4 ms), allowing carbon-carbon connectivities to be established.[57] This spectrum was recorded in less than 8 hours and displays excellent signal-to-noise ratio and resolution.

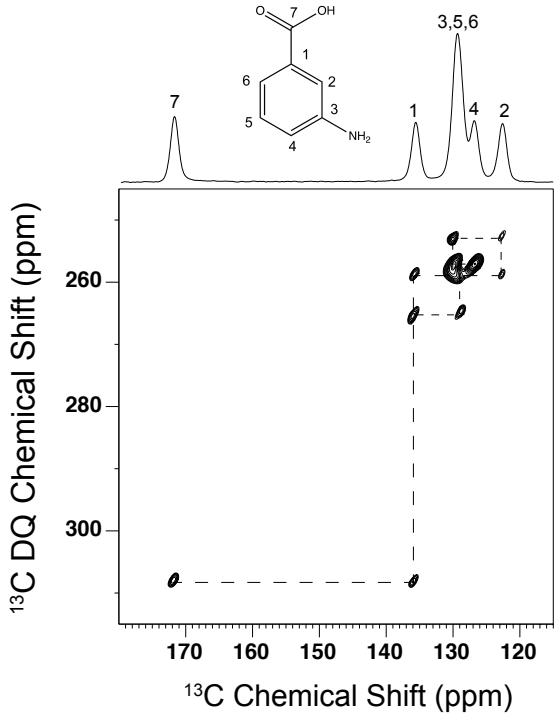

Figure 3: ^{13}C-^{13}C DQ/SQ dipolar correlation 2D spectrum recorded for a sample of natural abundance 3-aminobenzoic acid. The spectrum was recorded with microwave irradiation and for the powder

impregnated with a 80 mM solution of TEKPol in TCE. The dipolar recoupling time was adjusted to establish carbon-carbon connectivities.

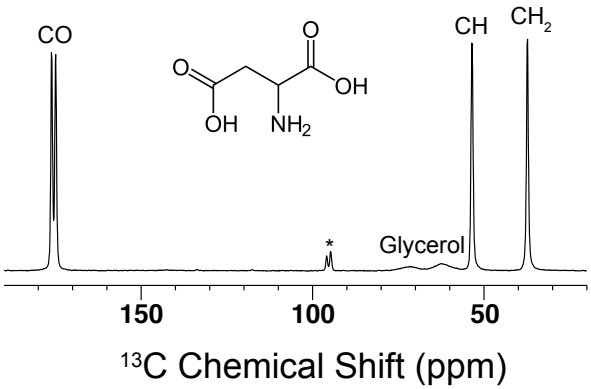

Figure 4: ^{1}H-^{13}C CP MAS spectra of L-aspartic acid at natural abundance recorded for the powder impregnated with a 45 mM solution of AMUPol in glycerol/D_2O/H_2O (60/30/10). The spectrum was recorded with microwave irradiation and at a temperature of 108 K. The experimental time to record the spectrum was 120 s. (The symbol * indicates a spinning side band)

Finally, it should be noted that the herein proposed solvent suppression method does not exclusively work with TCE. In fact, as examplified in Figure 4, similar results can be obtained for samples impregnated with a glycerol/water solution. In this case, a sample of L-aspartic acid at natural isotopic abundance was impregnated with a solution of 45 mM of AMUPol in glycerol/D_2O/H_2O (60/30/10). At a temperature of 108 K, two intense and broad ^{13}C resonances are usually observed at 72 and 62 ppm for the frozen glycerol.[56] In the spectrum shown in Figure 4, the intensity of the signals arising from glycerol were effectively reduced and are now more than 50 times less intense than the signals arising from L-aspartic acid. It should also be noted that the overall signal-to-noise ratio of the spectrum shown in Figure 4 is excellent, thanks to a DNP enhancement ε_{CP}=65 and a $T_1(^1H)$ of 16 s (estimated with a mono-exponential-fitting), and that the high resolution of the ^{1}H-^{13}C CP spectrum has been preserved.

3. Material and methods

Sample preparation

The L-aspartic sample acid at natural isotopic abundance was obtained from Sigma Aldrich and used without further purification. Several polymorphic forms exist for 3-aminobenzoic acid. Here we prepared and studied the polymorphic form III.[58] Before impregnation, the samples were finely ground by hand in a mortar and pestle for several minutes. The ^{1}H-^{13}C CPMAS spectra were inspected before and after grinding and impregnation to monitor a potential evolution of the polymorphic form III of 3-aminobenzoic acid; all ^{1}H-^{13}C CPMAS spectra were identical to the ^{1}H-^{13}C CPMAS spectrum reported by Hughes *et al.* for form III of 3-aminobenzoic acid. **[59]** The organic solvents utilized for impregnation were visually screened to evaluate whether the powder samples were insoluble.

The sample of 3-aminobenzoic acid (~ 40 mg) was impregnated with 20 μL of a solution of TEKPol in TCE/TCE-d_2 (20/80; v/v). Different concentrations of TEKPol were used and the concentration of 80 mM yielded optimal overall sensitivity enhancement (see Figure S2 of the Supporting Information). The PAs were dissolved in the desired solvent and no undissolved PA was observed by visual inspection of the solution. The wet powder was then mixed with a spatula and transferred to a sapphire rotor. The weight of the impregnated powder transferred into the rotor was 34 mg. Freeze−thaw (*i.e.* insert−eject) cycling did not lead to significant modifications of the ε_{CP} for the sample of 3-aminobenzoic acid.

For L-aspartic acid, 30 mg of powder was impregnated with 11 μL of a solution of 45 mM of AMUPol in glycerol-d_8/D_2O/H_2O (60/30/10; v/v/v); the weight of the impregnated powder transferred into the rotor was 29 mg.

NMR experiments

All DNP NMR experiments were recorded on a Bruker 9.4 T wide-bore magnet (400 and 100 MHz for the ^{1}H and ^{13}C Larmor frequency, respectively) operated by an AVANCE-III NMR spectrometer and equipped with a Bruker 3.2 mm low-temperature double-resonance DNP ^{1}H/^{29}Si/^{13}C CPMAS probe. The spectrometer was equipped with a gyrotron that allowed microwave (MW) irradiation of the sample. Specifically, the field sweep coil of the NMR magnet was set so that MW irradiation occurred at the maximum DNP enhancement of TOTAPOL (263.334 GHz). The estimated power of the MW beam at the output of the probe waveguide was 4 W.

The sample temperature was ~108 K for the ^{1}H-^{13}C CP MAS spectra recorded under microwave irradiation. The spinning frequency was set to 10 kHz for the experiments performed on 3-aminobenzoic acid and 8 kHz for the experiments performed on L-aspartic acid. The amplitude of the ^{1}H rf field was ramped during the contact time to improve efficiency. The recycle delay was 10 s and the CP contact time was 2.5 ms. The 1D spectra were were recorded with 4 repetitions and 2 dummy scans. The ^{1}H T_1 relaxation times were measured with the saturation/recovery pulse sequence and the ^{13}C cohenrece lifetimes (T_2') were measured using the CPMAS spin echo experiment.

The ^{13}C-^{13}C DQ/SQ dipolar correlation 2D spectrum was recorded using the $R20^{9}_{2}$ symmetry.[60, 61] The DQ excitation and reconversion delays were set to 0.4 ms in order to select dipolar ^{13}C-^{13}C couplings beteween covalently bonded ^{13}C–^{13}C spin pairs;[57] 37 t_1 increments and 96 repetions for each increment were used with a repetition delay of 4 s.

4. Conclusion

We have demonstrated that the signal of the solvent used for preparing DNP samples by incipient wetness impregnation can be conveniently quenched by paramagnetic relaxation using highly concentrated radical-containing solutions for impregnating the sample. This approach is compatible for both aqueous and organic solvents, and preserves the resolution of the spectrum and the overall sensitivity enhancement. Contrary to the other solvent suppression methodologies proposed previously, the method presented here does not require long dephasing times to suppress the signal of the solvent, and hence does not lead to signal loss for the sample under study. As a result, this methodology is suitable for the study of samples at natural isotopic abundance where maximal signal-to-noise ratios are sought.

5. Acknowledgement

We thank K. M. D Harris, C. E Hughes and A. Willamson for providing the polymoprphic form III of 3-aminobenzoic acid. We also thank Bruker SAS for access to the solid-state NMR spectrometer used here and Dr F. Aussenac and Dr P. Dorffer for experimental assistance. This study has received funding from the Excellence Initiative of Aix-Marseille University - A*Midex, a French “Investissements d’Avenir” programme supported of the A*MIDEX project (no. ANR-

11-IDEX-0001-02) funded by the "Investissements d'Avenir", and from the European Research Council (ERC) under the European Union's Horizon 2020 research and innovation programme (grant agreement No 758498).

6. References

1. Rossini, A. J.; Zagdoun, A.; Lelli, M.; Lesage, A.; Copéret, C.; Emsley, L., Dynamic Nuclear Polarization Surface Enhanced NMR Spectroscopy. *Acc. Chem. Res.* **2013,** *46* (9), 1942-1951.

2. Blanc, F.; Chong, S. Y.; McDonald, T. O.; Adams, D. J.; Pawsey, S.; Caporini, M. A.; Cooper, A. I., Dynamic Nuclear Polarization NMR Spectroscopy Allows High-Throughput Characterization of Microporous Organic Polymers. *J. Am. Chem. Soc.* **2013,** *135* (41), 15290-15293.

3. Mollica, G.; Le, D.; Ziarelli, F.; Casano, G.; Ouari, O.; Phan, T. N. T.; Aussenac, F.; Thureau, P.; Gigmes, D.; Tordo, P.; Viel, S., Observing Apparent Nonuniform Sensitivity Enhancements in Dynamic Nuclear Polarization Solid-State NMR Spectra of Polymers. *ACS Macro Lett.* **2014,** *3* (9), 922-925.

4. Lilly Thankamony, A. S.; Lion, C.; Pourpoint, F.; Singh, B.; Perez Linde, A. J.; Carnevale, D.; Bodenhausen, G.; Vezin, H.; Lafon, O.; Polshettiwar, V., Insights into the Catalytic Activity of Nitridated Fibrous Silica (KCC-1) Nanocatalysts from 15N and 29Si NMR Spectroscopy Enhanced by Dynamic Nuclear Polarization. *Angew. Chem. Int. Ed.* **2015,** *54* (7), 2190-2193.

5. Jantschke, A.; Koers, E.; Mance, D.; Weingarth, M.; Brunner, E.; Baldus, M., Insight into the Supramolecular Architecture of Intact Diatom Biosilica from DNP-Supported Solid-State NMR Spectroscopy. *Angew. Chem. Int. Ed.* **2015,** *54* (50), 15069-15073.

6. Geiger, Y.; Gottlieb, H. E.; Akbey, Ü.; Oschkinat, H.; Goobes, G., Studying the Conformation of a Silaffin-Derived Pentalysine Peptide Embedded in Bioinspired Silica using Solution and Dynamic Nuclear Polarization Magic-Angle Spinning NMR. *J. Am. Chem. Soc.* **2016,** *138* (17), 5561-5567.

7. Hirsh, D. A.; Rossini, A. J.; Emsley, L.; Schurko, R. W., 35Cl dynamic nuclear polarization solid-state NMR of active pharmaceutical ingredients. *Phys. Chem. Chem. Phys.* **2016,** *18* (37), 25893-25904.

8. Kobayashi, T.; Perras, F. A.; Goh, T. W.; Metz, T. L.; Huang, W.; Pruski, M., DNP-Enhanced Ultrawideline Solid-State NMR Spectroscopy: Studies of Platinum in Metal–Organic Frameworks. *J. Phys. Chem. Lett.* **2016,** *7* (13), 2322-2327.

9. Smith, A. N.; Long, J. R., Dynamic Nuclear Polarization as an Enabling Technology for Solid State Nuclear Magnetic Resonance Spectroscopy. *Anal. Chem.* **2016,** *88* (1), 122-132.

10. Mehler, M.; Eckert, C. E.; Leeder, A. J.; Kaur, J.; Fischer, T.; Kubatova, N.; Brown, L. J.; Brown, R. C. D.; Becker-Baldus, J.; Wachtveitl, J.; Glaubitz, C., Chromophore Distortions in Photointermediates of Proteorhodopsin Visualized by Dynamic Nuclear Polarization-Enhanced Solid-State NMR. *J. Am. Chem. Soc.* **2017,** *139* (45), 16143-16153.

11. Leskes, M.; Kim, G.; Liu, T.; Michan, A. L.; Aussenac, F.; Dorffer, P.; Paul, S.; Grey, C. P., Surface-Sensitive NMR Detection of the Solid Electrolyte Interphase Layer on Reduced Graphene Oxide. *J. Phys. Chem. Lett.* **2017,** *8* (5), 1078-1085.

12. Lilly Thankamony, A. S.; Wittmann, J. J.; Kaushik, M.; Corzilius, B., Dynamic nuclear polarization for sensitivity enhancement in modern solid-state NMR. *Prog. Nucl. Magn. Reson. Spectros.* **2017,** *102-103*, 120-195.

13. Sani, M.-A.; Martin, P.-A.; Yunis, R.; Chen, F.; Forsyth, M.; Deschamps, M.; O'Dell, L. A., Probing Ionic Liquid Electrolyte Structure via the Glassy State by Dynamic Nuclear Polarization NMR Spectroscopy. *J. Phys. Chem. Lett.* **2018,** *9* (5), 1007-1011.

14. Leroy, C.; Aussenac, F.; Bonhomme-Coury, L.; Osaka, A.; Hayakawa, S.; Babonneau, F.; Coelho-Diogo, C.; Bonhomme, C., Hydroxyapatites: Key Structural Questions and Answers from Dynamic Nuclear Polarization. *Anal. Chem.* **2017,** *89* (19), 10201-10207.

15. Caracciolo, F.; Paioni, A. L.; Filibian, M.; Melone, L.; Carretta, P., Proton and Carbon-13 Dynamic Nuclear Polarization of Methylated β-Cyclodextrins. *J. Phys Chem. B* **2018,** *122* (6), 1836-1845.

16. Rossini, A. J., Materials Characterization by Dynamic Nuclear Polarization-Enhanced Solid-State NMR Spectroscopy. *J. Phys. Chem. Lett.* **2018,** *9* (17), 5150-5159.

17. Gerfen, G. J.; Becerra, L. R.; Hall, D. A.; Griffin, R. G.; Temkin, R. J.; Singel, D. J., High frequency (140 GHz) dynamic nuclear polarization: Polarization transfer to a solute in frozen aqueous solution. *J. Chem. Phys.* **1995,** *102* (24), 9494-9497.

18. Ni, Q. Z.; Daviso, E.; Can, T. V.; Markhasin, E.; Jawla, S. K.; Swager, T. M.; Temkin, R. J.; Herzfeld, J.; Griffin, R. G., High Frequency Dynamic Nuclear Polarization. *Acc. Chem. Res.* **2013,** *46* (9), 1933-1941.

19. Bouleau, E.; Saint-Bonnet, P.; Mentink-Vigier, F.; Takahashi, H.; Jacquot, J. F.; Bardet, M.; Aussenac, F.; Purea, A.; Engelke, F.; Hediger, S.; Lee, D.; De Paëpe, G., Pushing NMR sensitivity limits using dynamic nuclear polarization with closed-loop cryogenic helium sample spinning. *Chem. Sci.* **2015,** *6* (12), 6806-6812.

20. Kemp, T. F.; Dannatt, H. R. W.; Barrow, N. S.; Watts, A.; Brown, S. P.; Newton, M. E.; Dupree, R., Dynamic Nuclear Polarization enhanced NMR at 187GHz/284MHz using an Extended Interaction Klystron amplifier. *J. Magn. Reson.* **2016,** *265*, 77-82.

21. Saliba, E. P.; Sesti, E. L.; Alaniva, N.; Barnes, A. B., Pulsed Electron Decoupling and Strategies for Time Domain Dynamic Nuclear Polarization with Magic Angle Spinning. *J. Phys. Chem. Lett.* **2018,** *9* (18), 5539-5547.

22. Can, T. V.; McKay, J. E.; Weber, R. T.; Yang, C.; Dubroca, T.; van Tol, J.; Hill, S.; Griffin, R. G., Frequency-Swept Integrated and Stretched Solid Effect Dynamic Nuclear Polarization. *J. Phys. Chem. Lett.* **2018,** *9* (12), 3187-3192.

23. Rosay, M.; Blank, M.; Engelke, F., Instrumentation for solid-state dynamic nuclear polarization with magic angle spinning NMR. *J. Magn. Reson.* **2016,** *264*, 88-98.

24. Thurber, K.; Tycko, R., Low-temperature dynamic nuclear polarization with helium-cooled samples and nitrogen-driven magic-angle spinning. *J. Magn. Reson.* **2016,** *264*, 99-106.

25. Matsuki, Y.; Idehara, T.; Fukazawa, J.; Fujiwara, T., Advanced instrumentation for DNP-enhanced MAS NMR for higher magnetic fields and lower temperatures. *J. Magn. Reson.* **2016,** *264*, 107-115.

26. Corzilius, B.; Smith, A. A.; Barnes, A. B.; Luchinat, C.; Bertini, I.; Griffin, R. G., High-Field Dynamic Nuclear Polarization with High-Spin Transition Metal Ions. *J. Am. Chem. Soc.* **2011,** *133* (15), 5648-5651.

27. Sauvée, C.; Rosay, M.; Casano, G.; Aussenac, F.; Weber, R. T.; Ouari, O.; Tordo, P., Highly Efficient, Water-Soluble Polarizing Agents for Dynamic Nuclear Polarization at High Frequency. *Angew. Chem. Int. Ed.* **2013,** *52* (41), 10858-10861.

28. Zagdoun, A.; Casano, G.; Ouari, O.; Schwarzwälder, M.; Rossini, A. J.; Aussenac, F.; Yulikov, M.; Jeschke, G.; Copéret, C.; Lesage, A.; Tordo, P.; Emsley, L., Large Molecular Weight Nitroxide Biradicals Providing Efficient Dynamic Nuclear Polarization at Temperatures up to 200 K. *J. Am. Chem. Soc.* **2013,** *135* (34), 12790-12797.

29. Mathies, G.; Caporini, M. A.; Michaelis, V. K.; Liu, Y.; Hu, K.-N.; Mance, D.; Zweier, J. L.; Rosay, M.; Baldus, M.; Griffin, R. G., Efficient Dynamic Nuclear Polarization at 800 MHz/527 GHz with Trityl-Nitroxide Biradicals. *Angew. Chem. Int. Ed.* **2015,** *54* (40), 11770-11774.

30. Bothe, S.; Nowag, J.; Klimavičius, V.; Hoffmann, M.; Troitskaya, T. I.; Amosov, E. V.; Tormyshev, V. M.; Kirilyuk, I.; Taratayko, A.; Kuzhelev, A.; Parkhomenko, D.; Bagryanskaya, E.; Gutmann, T.; Buntkowsky, G., Novel Biradicals for Direct Excitation Highfield Dynamic Nuclear Polarization. *J. Phys. Chem. C* **2018,** *122* (21), 11422-11432.

31. Geiger, M.-A.; Jagtap, A. P.; Kaushik, M.; Sun, H.; Stöppler, D.; Sigurdsson, S. T.; Corzilius, B.; Oschkinat, H., Efficiency of Water-Soluble Nitroxide Biradicals for Dynamic Nuclear Polarization in Rotating Solids at 9.4 T: bcTol-M and cyolyl-TOTAPOL as New Polarizing Agents. *Chemistry – A European Journal* **2018,** *24* (51), 13485-13494.

32. Mentink-Vigier, F.; Marin-Montesinos, I.; Jagtap, A. P.; Halbritter, T.; van Tol, J.; Hediger, S.; Lee, D.; Sigurdsson, S. T.; De Paëpe, G., Computationally Assisted Design of

Polarizing Agents for Dynamic Nuclear Polarization Enhanced NMR: The AsymPol Family. *J. Am. Chem. Soc.* **2018,** *140* (35), 11013-11019.

33. Wisser, D.; Karthikeyan, G.; Lund, A.; Casano, G.; Karoui, H.; Yulikov, M.; Menzildjian, G.; Pinon, A. C.; Purea, A.; Engelke, F.; Chaudhari, S. R.; Kubicki, D.; Rossini, A. J.; Moroz, I. B.; Gajan, D.; Copéret, C.; Jeschke, G.; Lelli, M.; Emsley, L.; Lesage, A.; Ouari, O., BDPA-Nitroxide Biradicals Tailored for Efficient Dynamic Nuclear Polarization Enhanced Solid-State NMR at Magnetic Fields up to 21.1 T. *J. Am. Chem. Soc.* **2018,** *140* (41), 13340-13349.

34. Mentink-Vigier, F.; Akbey, Ü.; Hovav, Y.; Vega, S.; Oschkinat, H.; Feintuch, A., Fast passage dynamic nuclear polarization on rotating solids. *J. Magn. Reson.* **2012,** *224*, 13-21.

35. Thurber, K. R.; Tycko, R., Perturbation of nuclear spin polarizations in solid state NMR of nitroxide-doped samples by magic-angle spinning without microwaves. *J. Chem. Phys.* **2014,** *140* (18), 184201.

36. Mentink-Vigier, F.; Akbey, Ü.; Oschkinat, H.; Vega, S.; Feintuch, A., Theoretical aspects of Magic Angle Spinning - Dynamic Nuclear Polarization. *J. Magn. Reson.* **2015,** *258*, 102-120.

37. Mance, D.; Gast, P.; Huber, M.; Baldus, M.; Ivanov, K. L., The magnetic field dependence of cross-effect dynamic nuclear polarization under magic angle spinning. **2015,** *142* (23), 234201.

38. Daube, D.; Aladin, V.; Heiliger, J.; Wittmann, J. J.; Barthelmes, D.; Bengs, C.; Schwalbe, H.; Corzilius, B., Heteronuclear Cross-Relaxation under Solid-State Dynamic Nuclear Polarization. *J. Am. Chem. Soc.* **2016,** *138* (51), 16572-16575.

39. Perras, F. A.; Sadow, A.; Pruski, M., In Silico Design of DNP Polarizing Agents: Can Current Dinitroxides Be Improved? *ChemPhysChem* **2017,** *18* (16), 2279-2287.

40. Hoffmann, M. M.; Bothe, S.; Gutmann, T.; Buntkowsky, G., Unusual Local Molecular Motions in the Solid State Detected by Dynamic Nuclear Polarization Enhanced NMR Spectroscopy. *J. Phys. Chem. C* **2017,** *121* (41), 22948-22957.

41. Kundu, K.; Feintuch, A.; Vega, S., Electron–Electron Cross-Relaxation and Spectral Diffusion during Dynamic Nuclear Polarization Experiments on Solids. *J. Phys. Chem. Lett.* **2018,** *9* (7), 1793-1802.

42. Takahashi, H.; Lee, D.; Dubois, L.; Bardet, M.; Hediger, S.; De Paëpe, G., Rapid Natural-Abundance 2D 13C–13C Correlation Spectroscopy Using Dynamic Nuclear Polarization Enhanced Solid-State NMR and Matrix-Free Sample Preparation. *Angew. Chem. Int. Ed.* **2012,** *51* (47), 11766-11769.

43. Rossini, A. J.; Widdifield, C. M.; Zagdoun, A.; Lelli, M.; Schwarzwälder, M.; Copéret, C.; Lesage, A.; Emsley, L., Dynamic Nuclear Polarization Enhanced NMR Spectroscopy for Pharmaceutical Formulations. *J. Am. Chem. Soc.* **2014,** *136* (6), 2324-2334.

44. Mollica, G.; Dekhil, M.; Ziarelli, F.; Thureau, P.; Viel, S., Quantitative Structural Constraints for Organic Powders at Natural Isotopic Abundance Using Dynamic Nuclear Polarization Solid-State NMR Spectroscopy. *Angew. Chem. Int. Ed.* **2015,** *54* (20), 6028-6031.

45. Smith, A. N.; Märker, K.; Piretra, T.; Boatz, J. C.; Matlahov, I.; Kodali, R.; Hediger, S.; van der Wel, P. C. A.; De Paëpe, G., Structural Fingerprinting of Protein Aggregates by Dynamic Nuclear Polarization-Enhanced Solid-State NMR at Natural Isotopic Abundance. *J. Am. Chem. Soc.* **2018,** *140* (44), 14576-14580.

46. Perras, F. A.; Wang, L.-L.; Manzano, J. S.; Chaudhary, U.; Opembe, N. N.; Johnson, D. D.; Slowing, I. I.; Pruski, M., Optimal sample formulations for DNP SENS: The importance of radical-surface interactions. *Current Opinion in Colloid & Interface Science* **2018,** *33*, 9-18.

47. Rossini, A. J.; Zagdoun, A.; Hegner, F.; Schwarzwälder, M.; Gajan, D.; Copéret, C.; Lesage, A.; Emsley, L., Dynamic Nuclear Polarization NMR Spectroscopy of Microcrystalline Solids. *J. Am. Chem. Soc.* **2012,** *134* (40), 16899-16908.

48. Pinon, A. C.; Schlagnitweit, J.; Berruyer, P.; Rossini, A. J.; Lelli, M.; Socie, E.; Tang, M.; Pham, T.; Lesage, A.; Schantz, S.; Emsley, L., Measuring Nano to Micro Structures from Relayed DNP NMR. *J. Phys. Chem. C* **2017**, *121*, 15993-16005.

49. Takahashi, H.; Hediger, S.; De Paëpe, G., Matrix-free dynamic nuclear polarization enables solid-state NMR 13C–13C correlation spectroscopy of proteins at natural isotopic abundance. *Chem. Commun.* **2013,** *49* (82), 9479-9481.

50. Le, D.; Casano, G.; Phan, T. N. T.; Ziarelli, F.; Ouari, O.; Aussenac, F.; Thureau, P.; Mollica, G.; Gigmes, D.; Tordo, P.; Viel, S., Optimizing Sample Preparation Methods for Dynamic Nuclear Polarization Solid-state NMR of Synthetic Polymers. *Macromolecules* **2014,** *47* (12), 3909-3916.

51. Kobayashi, T.; Perras, F. A.; Chaudhary, U.; Slowing, I. I.; Huang, W.; Sadow, A. D.; Pruski, M., Improved strategies for DNP-enhanced 2D 1H-X heteronuclear correlation spectroscopy of surfaces. *Solid State Nuclear Magnetic Resonance* **2017,** *87*, 38-44.

52. Yarava, J. R.; Chaudhari, S. R.; Rossini, A. J.; Lesage, A.; Emsley, L., Solvent suppression in DNP enhanced solid state NMR. *J. Magn. Reson.* **2017,** *277*, 149-153.

53. Lee, D.; Chaudhari, S. R.; De Paëpe, G., Solvent signal suppression for high-resolution MAS-DNP. *J. Magn. Reson.* **2017,** *278*, 60-66.

54. Hall, D. A.; Maus, D. C.; Gerfen, G. J.; Inati, S. J.; Becerra, L. R.; Dahlquist, F. W.; Griffin, R. G., Polarization-Enhanced NMR Spectroscopy of Biomolecules in Frozen Solution. *Science* **1997,** *276* (5314), 930.

55. Kobayashi, T.; Slowing, I. I.; Pruski, M., Measuring Long-Range 13C–13C Correlations on a Surface under Natural Abundance Using Dynamic Nuclear Polarization-Enhanced Solid-State Nuclear Magnetic Resonance. *J. Phys. Chem. C* **2017,** *121* (44), 24687-24691.

56. Pinon, A. C.; Rossini, A. J.; Widdifield, C. M.; Gajan, D.; Emsley, L., Polymorphs of Theophylline Characterized by DNP Enhanced Solid-State NMR. *Mol. Pharm.* **2015,** *12* (11), 4146-4153.

57. Dekhil, M.; Mollica, G.; Bonniot, T. T.; Ziarelli, F.; Thureau, P.; Viel, S., Determining carbon–carbon connectivities in natural abundance organic powders using dipolar couplings. *Chem. Commun.* **2016,** *52* (55), 8565-8568.

58. Williams, P. A.; Hughes, C. E.; Lim, G. K.; Kariuki, B. M.; Harris, K. D. M., Discovery of a New System Exhibiting Abundant Polymorphism: m-Aminobenzoic Acid. *Cryst. Growth Des.* **2012,** *12* (6), 3104-3113.

59. Hughes, C. E.; Williams, P. A.; Harris, K. D. M., "CLASSIC NMR": An In-Situ NMR Strategy for Mapping the Time-Evolution of Crystallization Processes by Combined Liquid-State and Solid-State Measurements. *Angew. Chem. Int. Ed.* **2014,** *53* (34), 8939-8943.

60. Carravetta, M.; Edén, M.; Johannessen, O. G.; Luthman, H.; Verdegem, P. J. E.; Lugtenburg, J.; Sebald, A.; Levitt, M. H., Estimation of Carbon–Carbon Bond Lengths and Medium-Range Internuclear Distances by Solid-State Nuclear Magnetic Resonance. *J. Am. Chem. Soc.* **2001,** *123* (43), 10628-10638.

61. Edén, M., *Advances in Symmetry-Based Pulse Sequences in Magic-Angle Spinning Solid-State NMR*. John Wiley & Sons, Ltd: 2013; Vol. 2.